RSC Advances

PAPER

View Article Online
View Journal | View Issue

Cite this: *RSC Adv.*, 2016, **6**, 31861

Asymmetric tandem hemiaminal-heterocyclization-aza-Mannich reaction of 2-formylbenzonitriles and amines using chiral phase transfer catalysis: an experimental and theoretical study†

Amedeo Capobianco,*[a] Antonia Di Mola,[a] Valentina Intintoli,[a] Antonio Massa,[a] Vito Capaccio,[a] Lukas Roiser,[b] Mario Waser[b] and Laura Palombi*[a]

Received 1st March 2016
Accepted 22nd March 2016

DOI: 10.1039/c6ra05488a

www.rsc.org/advances

The first asymmetric synthesis of 3-amino-substituted isoindolinones was accomplished *via* cascade hemiaminal-heterocyclization-intramolecular aza-Mannich reaction of benzylamines and 2-formylbenzonitriles using chiral phase transfer conditions (PTC). A theoretical study of the enantioselective step provides a rationale for the mode of action of the best performing phase transfer catalyst and the observed face selectivity.

Introduction

The 3-substituted-isoindolin-1-one framework belongs to a class of heterocyclic substructures which occurs in various natural and synthetic biologically active compounds.[1] The isoindolinonic chiral core is present, for example, in the active part of commercially available pazinaclone, pagoclone and zopiclone, drugs that find applications as sedative-hypnotic agents.[2] Isoindolinone nucleus is also found in natural and synthetic products with therapeutic applications in neurological disorders like Parkinson and Alzheimer diseases, as well as in the treatment of cancer, cardiac arrhythmia and HIV.[3] Therefore, the interest in the construction of heterocycles based on the isoindolinonic ring is steadily increasing as testified by the large number of recent reports dealing with this subject.[4]

In order to have small collections of potentially bioactive molecules focused on this heterocyclic architecture, in last years, we have also addressed research efforts in their achievement from readily available starting material 2-formylbenzonitriles using chemical[5] or electrochemical[6] strategies which enable tandem processes to directly access the molecular target.

In particular, we have recently demonstrated the possibility to induce the title reaction under electrochemical conditions, thus incorporating an interesting α-amino amidic functionality in the isoindolinonic ring.[7]

Furthermore, the product has been smoothly obtained in our laboratories, by simple treatment of the reactants with a stoichiometric amount of K_2CO_3 in CH_3CN. In this case, as evidenced in Scheme 1 for a generic primary amine RNH_2, the reaction should proceed by a sequence of hemiaminal formation (a), a base catalyzed heterocyclization step (b) and a subsequent rearrangement *via* an uncommon aza-Mannich reaction (c).

With the understanding of the basic principles of this chemistry in hand, we became interested to design an asymmetric version of this reaction, relying on the assumption that, under liquid–solid phase transfer conditions (*i.e.* organic solvent/inorganic base), chiral ammonium catalysts[8] could help

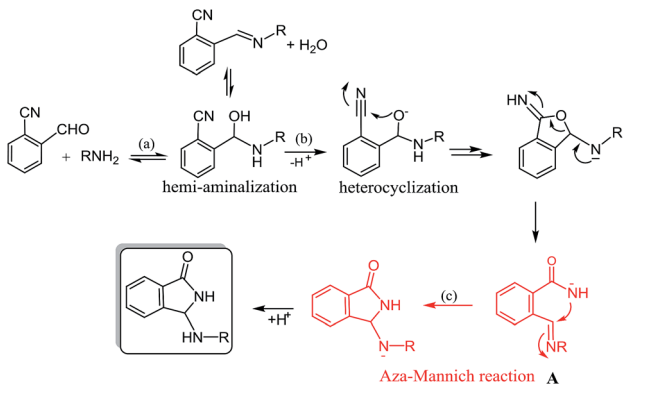

Scheme 1 Reaction pathway for the reaction of 2-formybenzonitriles and primary amines.

[a]*Dipartimento di Chimica e Biologia, Università di Salerno, Via Giovanni Paolo II, I-84084, Fisciano (SA), Italy. E-mail: acapobianco@unisa.it; lpalombi@unisa.it*

[b]*Institute of Organic Chemistry, Johannes Kepler University Linz, Altenberger Strasse 69, 4040 Linz, Austria*

† Electronic supplementary information (ESI) available. See DOI: 10.1039/c6ra05488a

in the enantioselective construction of the chiral center during the rearrangement step.

In fact, the use of chiral-onium salts as phase transfer catalysts[9] dates back a long time ago, nevertheless current research papers still provide new insights on this subject, both by reporting new potential uses in asymmetric synthesis[10] and by offering explanations on their action mechanism.[11]

Herein we demonstrate the first asymmetric access to 3-amino-substituted isoindolinones *via* base catalyzed intramolecular aza-Mannich reaction, under chiral phase transfer conditions.

Results and discussion

In a first investigation (Table 1), to assess the effectiveness of the reaction, benzylamine and *o*-cyanobenzaldehyde were reacted in the presence of inorganic base K_2CO_3, using the series of ammonium salts listed in Fig. 1.[12]

Compared with classical monofunctional ammonium salts (**III**, **V**), bifunctional derivatives with a H-bonding donor (**II**, **IV**, **VI**, **VII**, **VIII**) show an improved catalytic activity (resulting in a higher conversion in shorter reaction times), while the presence of a bulky, rigidifying substituent on the nitrogen atom (*i.e.* 9-anthracenylmethyl group), appears to be crucial to achieve an increase in enantioselectivity. Despite many attempts have been made to optimize the reaction (choice of the solvent and base, different biphasic conditions, reactants and catalyst loading, change in temperature *etc.*, see Chart 1 in the ESI†), the enantioselectivity was lying on modest levels with a maximum of 78/22 e.r. achieved under the conditions reported in Table 1, entry 15.

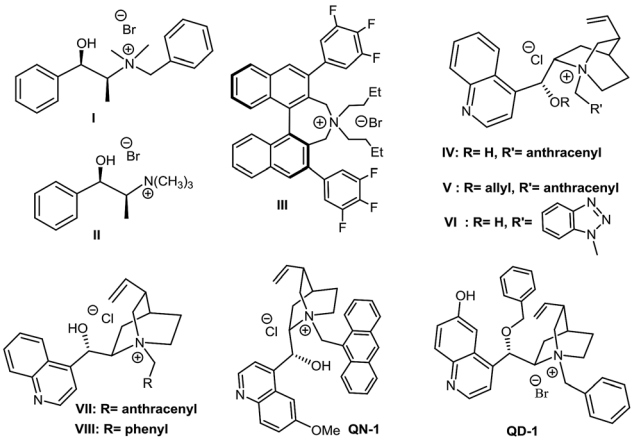

Fig. 1 First screening of chiral ammonium salts tested in this work.

Although under phase transfer conditions, the stereocontrol usually derives from the electrostatic attraction of opposite charged species, several studies demonstrated that a further coordination *via* multiple noncovalent interactions (similarly to bifunctional organobase-H-bonding catalysts) may significantly enhance the catalyst performance in many cases.[13] Based on the above observations, we decided to test the catalytic ability of ammonium salts having additional hydrogen-bonding sites (Fig. 2).[14]

While Dixon's ammonium salt **IX** [10d] (Table 2, entry 1) performed the same way as catalysts of Table 1, placing the hydrogen-bond donor on the quinoline ring resulted in a substantial increase of enantioselectivity, **QNOH-1** reaching the best enantiomeric ratio under optimized conditions (Table 2, entries 7 and 8).

Furthermore, whereas ammonium salts **QNOH-2** or **QNOH-3** with different substituents on nitrogen atom gave comparable enantioselectivities, the crucial importance to have both the –OH functionalities emerges by comparison with the catalysts **QN-1** and **QD-1** which led to the expected product with low or vanishing enantiomeric excesses (Table 1, entries 6 and 7).

Table 1 Tandem reaction of **1a** with **2a** under PTC conditions: initial screening of the common catalysts listed in Fig. 1

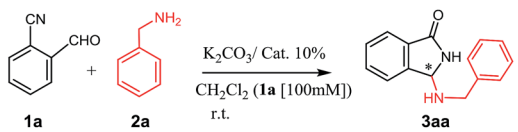

Entry	Catalyst (% mol)	Time (h)	Yield[a] (%)	E.r.[b]
1	**I** (10)	3	88	55/45
2	**II** (10)	3	88	56/46
3	**IV** (10)	3	96	57/43
4	**V** (10)	32	71	57/43
5	**QD-I** (10)	18	75	51/49
6	**QN-I** (10)	18	85	60/40
7[c]	**VI** (10)	1	65	56/44
8[c,d]	**VI** (10)	3	92	60/40
9[c]	**III** (10)	18	92	40/60
10[c]	**IV** (10)	1	86	65/35
11[c]	**IV** (5)	1	54	72/28
12[d,e]	**IV** (10)	15	81	64/36
13[c,d]	**VII** (10)	8	92	32/68
14[c,d]	**VIII** (10)	18	90	60/40
15[c,d]	**IV** (10)	8	86	78/22

[a] Yields refer to isolated products. [b] E.r. determined by HPLC using a chiral stationary phase. [c] Reaction performed in toluene, **1a** [50 mM]. [d] Reaction temperature: −20 °C. [e] Reaction performed in xylene, **1a** [50 mM].

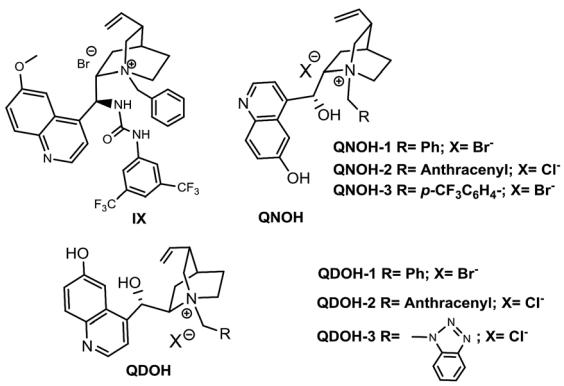

Fig. 2 Multiple H-bonding donor containing chiral ammonium salts tested in this work.

Table 2 Tandem reaction of **1a** with **2a** under PTC conditions: screening of the catalysts listed in Fig. 2

Entry	Catalyst (% mol)	Yields[a] (%)	E.r.[b]
1[c]	**IX** (10)	92	39/61
2[c]	**QDOH-1** (12)	85	24/76
3[c]	**QDOH-1** (6)	85	24/76
4	**QDOH-1** (8)	89	15/85
5	**QDOH-2** (8)	84	12/88
6	**QDOH-3** (8)	72	15/85
7[c]	**QNOH-1** (8)	92	87/13
8	**QNOH-1** (8)	**92**	**93/7 (99/1)**[d]
9	**QNOH-2** (10)	92	92/8
10	**QNOH-3** (10)	92	92/8

[a] Yields refer to isolated products. [b] E.r. determined on HPLC equipped with chiral column. [c] Toluene was used as solvent, 8 h, r.t. [d] Nearly enantiopure **3aa** was easily accessed through a reverse crystallization process from DCM/hexane solution.[15] Indeed, as reported by us for other 3-substituted isoindolinones,[5b] the preferential formation of heterocrystals containing (*R*) and (*S*)-enantiomers, allowed the enantiomeric enrichment of mother liquor from the original non-racemic solution.

Finally, it is worthy to note that the pseudo enantiomeric **QDOH** catalysts allowed an effective inversion of enantioselectivity which is not always observed with the first series of catalysts (Table 1, entry 14). Subsequently, the scope of the tandem process has been expanded to a variety of 2-formylbenzonitriles (**1**) and amines (**2**), using the most successful conditions obtained in Table 2, entry 7. As reported in Table 3, 2-formylbenzonitrile derivatives **1a–e** with both electron-donating groups and electron-withdrawing groups smoothly reacted with primary amines **2a–d** generating **3** in very good yields and ees (up to 90%). Noteworthy, an appreciable enantiomeric excess has been also obtained with aliphatic amine **2d**.

Table 3 Tandem reaction of **1** with **2** using catalyst **QNOH-1**[a]

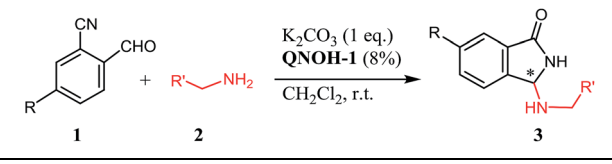

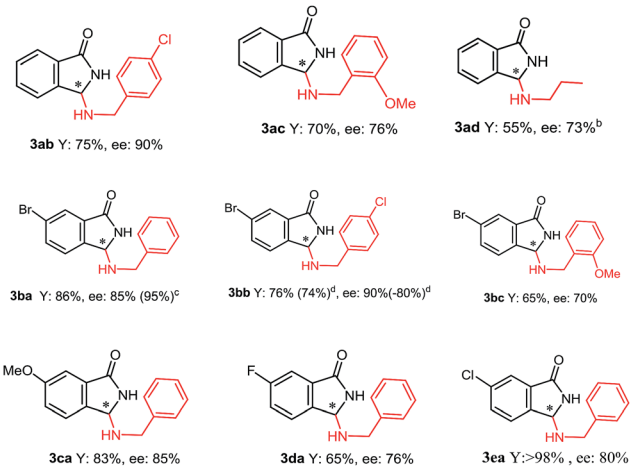

[a] Experimental conditions: unless otherwise indicated, see entry 7, Table 2. [b] Catalyst loading 10%. Reaction time: 48 h, conversion 60%. [c] In parentheses ee after reverse crystallization. [d] In parentheses yield and ee obtained with the catalyst **QDOH-1**.

Mechanism

Given these interesting results, to unravel the origin and the sense of the asymmetric induction, we have investigated the enantioselective step of the reaction of **1a** with **2a** (*i.e.* the aza-Mannich reaction) by quantum chemical computations.

Our study started by analyzing the conformer distribution of the cinchona alkaloid-derivative ammonium cation **QNOH-1** and the **A** intermediate involved in the rearrangement step. In line with previous results,[16] the ammonium cation is predicted to assume *open* conformations at 298 K with a preference for the anti orientation (see Fig. S1 and Table S1 in the ESI†), the closed forms being ruled out by unfavorable steric interactions between the benzyl and quinoline moieties.

All the bonds of the **A** intermediate were allowed to be rotatable in docking simulations. In this way also the possibility of the *Z* configuration was considered for the binary complexes formed by the **A** intermediate and the ammonium catalyst. Sampling the full conformational space of such a highly flexible system was a necessary effort to make sure that the most significant arrangements for the **A:QNOH-1** ion-pairs were actually located (see Table S2 in the ESI†).[17]

Because of the large size of the system, a plethora of binary complexes between the **QNOH-1** ammonium and the **A** intermediate has to be expected and indeed 74 unique complexes were found by DFT computations (Tables S3 and S4 of the ESI†). Moreover the presence of two hydroxyl donor groups on the catalyst and three acceptor units on the **A** intermediate gives rise to a wide panel of association modes. The most populated binary complexes are characterized by two hydrogen bonds, according to the coordination patterns exemplified by ***Ia*1** (and ***Ia*2**), ***Ib*1** (and ***Ib*2**), ***Ic*** and ***Id*** reactant complexes of Fig. 3 (a, b, c and d denote the hydrogen bonds patterns; additional arrangements are reported in Fig. S2 of the ESI†). In ***Ia*1** and its nearly isoenergetic homologue ***Ia*2** (see Table S5 in the ESI†) the nucleophilic nitrogen of intermediate **A** is engaged in a H bond with the hydroxyl at the C^9 of **QNOH-1** while the iminic nitrogen holds the hydroxyl at the $C^{6'}$. An opposite coordination is found for ***Ic***; here the C^9 hydroxyl holds the iminic nitrogen while the $C^{6'}$ hydroxyl coordinates the nucleophilic nitrogen of **A**. Both the *E* configuration of **A** and the open conformation of the catalyst are retained in ***Ia*1**, ***Ia*2** and ***Ic*** (Fig. 4).

They are strongly associated ion-pairs further stabilized by hydrogen bonds and π–π stacking interactions between the aromatic moiety of the intermediate and the quinoline ring of the catalyst. ***Ia*1** is slightly favored over ***Ic*** due to a T-shaped CH–π interaction involving the phenyl rings of **A** and **QNOH-1** (Fig. 4).

Starting from ***Ia*1**, ***Ia*2**, and ***Ic***, a torsion of 180° about the C–C′ bond (Fig. 3) generates ***Ib*1**, ***Ib*2** and ***Id***, respectively, in which the carbonyl oxygen replaces the nucleophilic nitrogen as the acceptor. ***Ib*1**, ***Ib*2** and ***Id*** rather than ***Ia*1**, ***Ia*2** and ***Ic*** are the

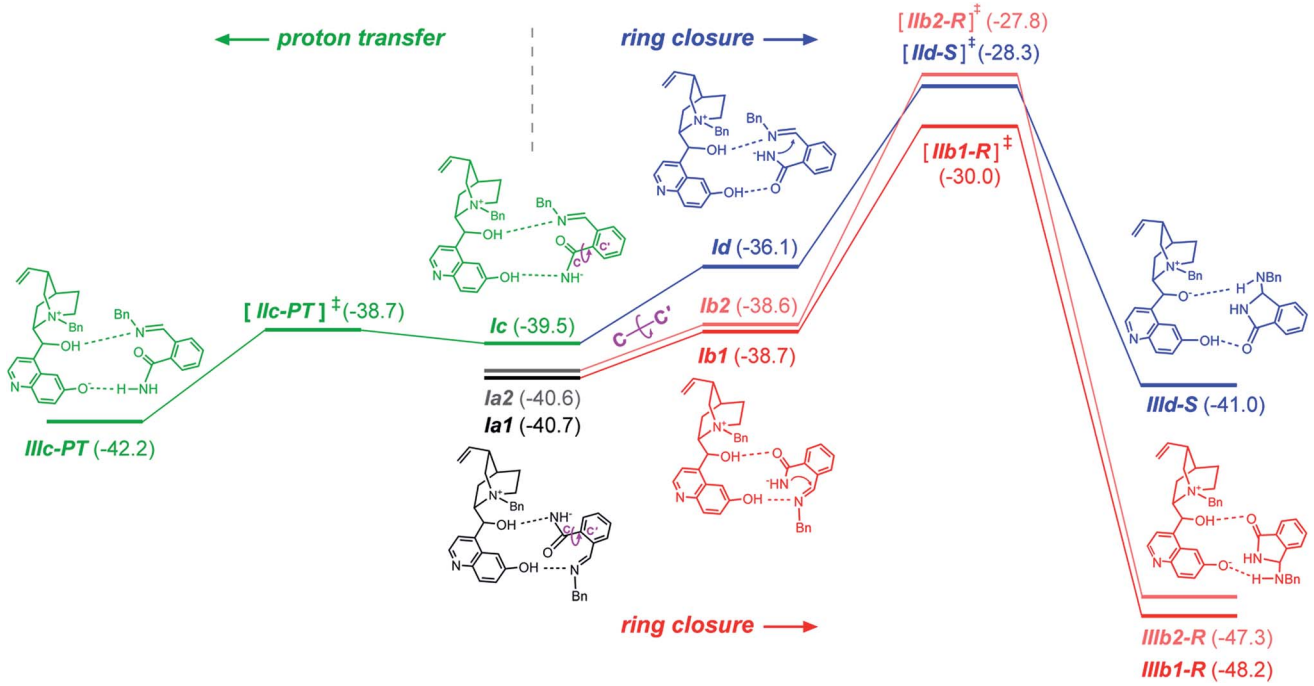

Fig. 3 Schematic energy profile of the enantioselective ring closure step (red and blue) and proton transfer (green). Relative energy (kcal mol^{-1}) refers to non-interacting A intermediate and QNOH-1 ammonium cation.

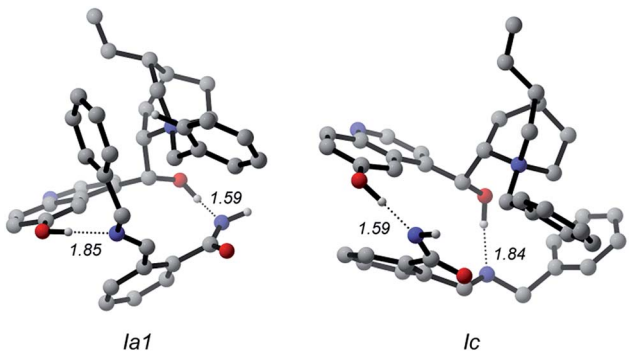

Fig. 4 The most stable binary complexes of the A intermediate and QNOH-1 cation for a and c patterns. Noncritical hydrogen atoms omitted for clarity. Distances in Å.

actual reactive complexes for the ring closure process, because in ***Ib*1**, ***Ib*2** and ***Id*** the nucleophilic nitrogen comes into close contact with the electrophilic carbon (Fig. 3). Indeed, following the reaction coordinate for the ring-closure, ***Ib*1** and ***Ic*** evolve into ***IIb*1-*R*** and ***IId-S*** transition states in which an incipient formation of the C–N bond occurs, as revealed by the shortening of the C–N distance, which amounts to *ca.* 3 Å in ***Ib*1** and 1.9 Å in ***IIb*1-*R*** (Fig. 5).

IIb*1-*R and ***IId-S*** are predicted to be the most stable among all pro-*R* and pro-*S* transition states, (see Table S3 in the ESI†). ***IIb*1-*R*** is more stable than ***IId-S*** by 1.7 kcal mol^{-1} (Fig. 3) implying an easier accessibility for the *R* configuration of the product. This is confirmed by a statistical analysis considering all the transition states (see Table S3 of ESI†) which gives an 86% ee in favor of the *R* enantiomer, in very good agreement with the observed excess. The nucleophilic attack is accompanied by an increase of negative charge on the imine nitrogen

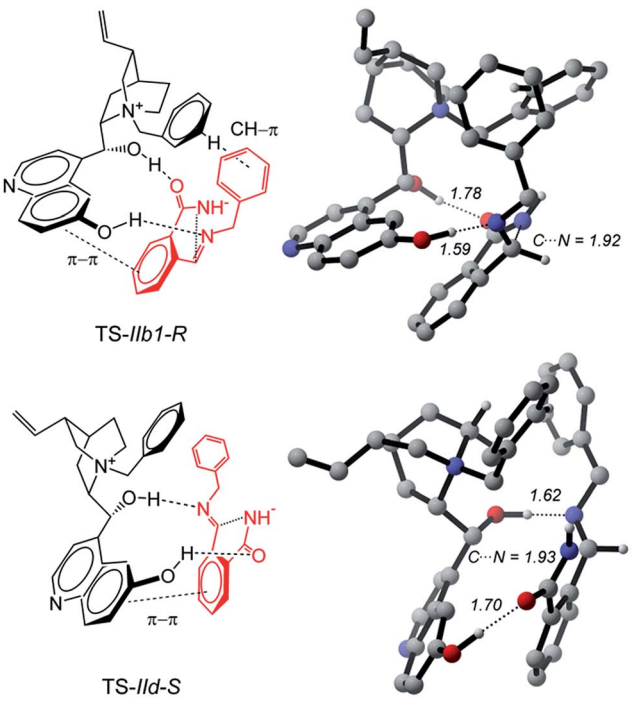

Fig. 5 Energetically most accessible transition states leading to the *R* and *S* enantiomers of product **3aa**. Noncritical hydrogen atoms omitted for clarity. Distances in Å.

(step b of Scheme 1). This is confirmed by computations: the APT charge of the imine nitrogen charge passes from −0.9 in ***Ib*1** and ***Id*** to −1.4 in ***IIb*1-*R*** and ***IId-S*** thus showing that the proton involved in the O–H···N hydrogen bond greatly facilitates the ring closure step.

Therefore, the different stability of the transition states can be traced back to the different patterns of hydrogen bonds. In fact it becomes relevant whether the quinoline OH or the C^9 hydroxyl of the catalyst acts as the donor in the OH···N bond because the Lewis basicity of the imine moiety of **A** in the transition state is supported by a quite strong phenol-like acidic function in the former case (***IIb*1-*R***), while a much weaker acidic hydroxyl is involved in the latter case (***IId-S***). Following the intrinsic reaction coordinate, ***IIb*1-*R*** and ***IId-S*** evolve into ***IIIb*1-*R*** and ***IIId-S*** product complexes, where the C–N bond is fully established. Very interestingly, the ring closure is predicted to proceed in concert with a proton transfer from the ammonium catalyst to the imine nitrogen, in such way that the final product **3** is directly obtained and the ammonium catalyst is converted into its corresponding betaine (Fig. 6). This strongly suggests that the initial base activator is indeed the betaine species, whose occurrence can be reasonably expected due to the acidity of **QNOH-1** ammonium and the presence of carbonate.[18]

The final step is thermodynamically favored for the pathway leading to *R* product, ***IIIb*1-*R*** being 7.5 kcal mol^{-1} more stable than ***Ia*** (Fig. 3). At variance with ***IIIb*1-*R*** where the proton transfer involves the acidic phenol hydroxyl of quinoline, in ***IIId-S*** deprotonation of **QNOH-1** ammonium occurs on C^9 hydroxyl, making the ring formation for the *S*-configured product a less affordable process.

We have also considered the possibility of a direct acid–base reaction between the rather acidic **QNOH-1** cation and intermediate **A**. That product would lead to the amide depicted in Fig. 3 (bottom left, green bars). First of all (see Fig. S2 in the ESI†), proton transfer is predicted to be a viable process only for ***Ic*** (Fig. 3) because only there the most acidic function of the catalyst can interact with the most basic function of the **A** intermediate. From ***Ic*** a proton transfer from **QNOH-1** to **A** could result into ***IIIc-PT*** product complex in which amide is coordinated to the betaine. However a glance at Fig. 3 (green bars, bottom left) will show that formation of the amide, although kinetically feasible, would lead to a very modest energy gain (1.5 kcal mol^{-1}) in comparison with the ring closure process (7.5 kcal mol^{-1}). In addition, the occurrence of two affordable and nearly isoenergetic pathways (dark and light red, Fig. 3) leading to the ring closure for the *R* product further favours the formation of product ***III***.

In summary the theoretical investigation confirms the expectations of the design process, stressing the fundamental role of the hydroxyls on selectivity: the presence of two OH groups makes the catalyst a bifunctional promoter capable of orienting the intermediate **A** in a preferential way through the establishment of an effective network of hydrogen bonds, which happens to facilitate the *R*-configured product.

On the bases of available evidence[18] and DFT results we can assume that, after the initial hemi-aminalization, the catalytic cycle should start with an acid–base reaction between the ammonium cation and CO_3^{2-} with the generation of the ammonium betaine assisting the heterocyclization and/or the rearrangement step by H-bonding catalysis. The rearrangement step produces the structured intermediate **A**/ammonium cation ion-pair that undergoes the asymmetric aza-Mannich reaction. The asymmetric step leads to the final product **3** regenerating the betaine catalyst (Scheme 2).

Assignment of the absolute configuration of the product

Since various attempts to crystallize product **3aa** failed, in order to assess the absolute configuration of the major enantiomer, the chiral amines (*S*)-**2f** and (*R*)-**2f** were reacted with **1a** in the presence of **QNOH-1** as catalyst (Fig. 7).

As evidenced by the NMR spectra on the crude mixtures, (*S*)-**2f** and (*R*)-**2f** yielded the product **3af** with reverse diastereoselectivity, thus implying the same configuration at the newly created stereogenic center. Moreover, in both cases, the diastereoselectivity is comparable to the enantioselectivity obtained with achiral benzylamine **2a**. On the contrary, a nearly 1 : 1 mixture of diastereoisomers is obtained under non-asymmetric reaction conditions. These results let us deduce that, also with chiral amines, the stereocontrol is totally due to the catalyst and, as a consequence, the absolute configuration of **3aa** can be confidently attributed on the base of the configurations of **3af**. The relative configurations of the two diastereoisomers **3af** were deduced from the ^{1}H NMR spectra which were assigned with the aid of computations. The chemical shift

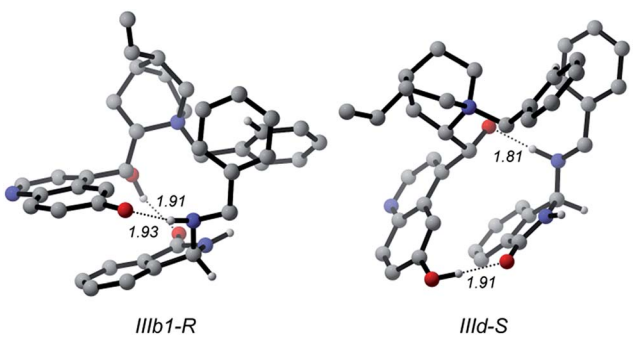

Fig. 6 *R* and *S* enantiomers of the final product coordinated to betaine. Noncritical hydrogen atoms omitted for clarity. Distances in Å.

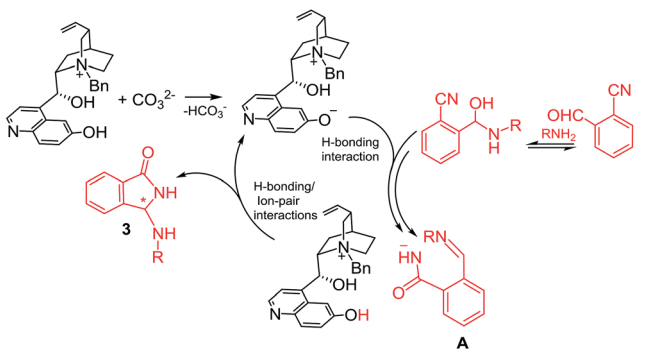

Scheme 2 Comprehensive catalytic cycle.

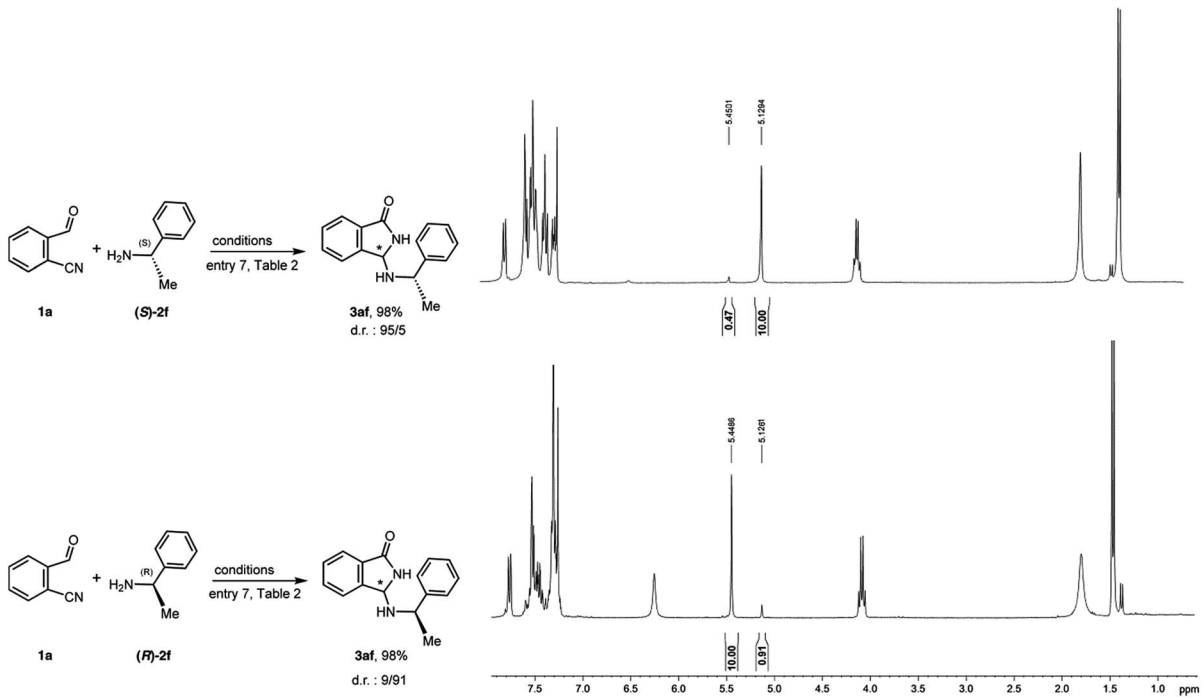

Fig. 7 Reaction of **1a** with chiral amines (*S*)-**2f** and (*R*)-**2f** under phase transfer conditions and relative ^{1}H-NMR spectra of the diastereomeric mixtures.

of the H atom on the isoindolinonic ring is predicted to be 5.42 ppm for the diastereoisomer (*RR*,*SS*) and 5.05 ppm for the diastereomer (*SR*,*RS*).

Taking advantage from the known configuration of the chiral starting amines, the comparison with the experimental spectra ($\delta = 5.45$ ppm and 5.13 ppm) unequivocally shows that the new formed stereocenter possesses *R* configuration.

This strongly suggests that the most abundant enantiomer of compound **3aa** also possesses *R* configuration, as anticipated by DFT predictions.

Experimental

For detailed experimental information, spectra and chromatograms of all the new compounds see the ESI.† Catalysts **I**, **II**, **III**, **IV**, **V** and **VII** are commercially available. Catalysts **VI**,[19] **QN1**,[13a] **QD1** (ref. 20) and **IX** [10d] have been prepared in accordance with the literature and gave spectral and analytical data as reported.

General procedure for the synthesis of bifunctional chiral phase transfer catalysts QDOH-1, QDOH-2, QNOH-1, QNOH-2, QNOH-3

All the ammonium salts were prepared by following the reported procedure for the quaternisation of tertiary amines[13a] from 6′-demethylated quinine (catalyst **QNOH**) and 6′-demethylated quinidine (catalyst **QDOH**) which were prepared as reported in the literature.[21]

Catalyst QNOH-1. Catalyst **QNOH-1**: by following the general procedure, starting from 6′-demethylated quinine (316 mg, 0.98 mmol) and benzyl bromide (128 μL, 184 mg, 0.98 mmol). Beige solid, (350 mg, 0.73 mmol, 74%). Mp > 200 °C; $[\alpha]_D = -206.6°$ ($c = 1.0$, MeOH, 23 °C); ^{1}H NMR (500 MHz, CD_3OD, 298.0 K, δ [ppm]): 1.45–1.52 (m, 1H), 1.84–1.92 (m, 1H), 2.06–2.10 (m, 1H), 2.23–2.29 (m, 1H), 2.29–2.36 (m, 1H), 2.68–2.75 (m, 1H), 3.35–3.43 (m, 1H), 3.46–3.53 (m, 1H), 3.56–3.62 (m, 1H), 3.92–3.98 (m, 1H), 4.37–4.45 (m, 1H), 4.92 (d, $J = 12.3$ Hz, 1H), 5.04 (dd, $J_{AC} = 10.5$ Hz, $J_{AB} = 1.2$ Hz, 1H), 5.17 (dd, $J_{BC} = 17.1$ Hz, $J_{AB} = 1.2$ Hz, 1H), 5.22 (d, $J = 12.3$ Hz, 1H), 5.72 (ddd, $J_{BC} = 17.1$ Hz, $J_{AC} = 10.5$ Hz, $J_{CX} = 6.9$ Hz, 1H), 6.49 (s, 1H), 7.43 (dd, $J = 2.5$ Hz, $J = 9.1$ Hz, 1H), 7.47 (d, $J = 2.4$ Hz, 1H), 7.58–7.62 (m, 3H), 7.70–7.75 (m, 2H), 7.85 (d, $J = 4.6$ Hz, 1H), 7.99 (d, $J = 9.1$ Hz, 1H), 8.73 (d, $J = 4.6$ Hz, 1H); ^{13}C NMR (125 MHz, MeOD, 298.0 K, *d* [ppm]): 22.9, 26.6, 28.8, 39.9, 53.3, 62.6, 66.2, 66.8, 70.5, 105.5, 118.2, 121.9, 124.0, 128.2, 129.3, 131.1 (2C), 132.5, 132.7, 135.6 (2C), 139.4, 144.7, 146.1, 148.4, 158.7; IR (ATR): 3217, 1620, 1530, 1465, 1216, 925, 861, 832, 766, 719, 706 cm^{-1}; HRMS (API) calcd for $[C_{26}H_{29}N_2O_2^+]$ 401.2224, found 401.2216.

Catalyst QNOH-2. Catalyst **QNOH-2**: by following the general procedure, starting from 6′-demethylated quinine (334 mg, 1.08 mmol) and 4-(trifluoromethyl)benzyl bromide (184 μL, 284 mg, 1.19 mmol). Beige solid (462 mg, 0.84 mmol, 78%). Mp > 200 °C; $[\alpha]_D = -48.4°$ ($c = 0.5$, MeOH, 23 °C); ^{1}H NMR (500 MHz, MeOD, 298.0 K, δ [ppm]): 1.43–1.51 (m, 1H), 1.83–1.91 (m, 1H), 2.06–2.10 (m, 1H), 2.22–2.28 (m, 1H), 2.28–2.35 (m, 1H), 2.68–2.74 (m, 1H), 3.29–3.31 (m, 1H), 3.45–3.51 (m, 1H), 3.62–3.68 (m, 1H), 3.94–4.00 (m, 1H), 4.41–4.49 (m, 1H), 5.03 (d, $J = 12.4$ Hz, 1H), 5.04 (dd, $J_{AC} = 10.3$ Hz, $J_{AB} = 1.2$ Hz, 1H), 5.17 (dd, $J_{BC} = 17.2$ Hz, $J_{AB} = 1.2$ Hz, 1H), 5.29 (d, $J = 12.4$ Hz, 1H), 5.72 (ddd, $J_{BC} = 17.1$ Hz, $J_{AC} = 10.5$ Hz, $J_{CX} = 6.9$ Hz, 1H), 6.48 (s, 1H), 7.41 (dd, $J = 2.5$ Hz, $J = 9.1$ Hz, 1H), 7.45–7.47 (m, 1H), 7.84 (d, $J = 4.6$

Hz, 1H), 7.89 (d, J = 8.2 Hz, 2H), 7.95 (d, J = 8.2 Hz, 2H), 7.98 (d, J = 9.1 Hz, 1H), 8.72 (d, J = 4.6 Hz, 1H); ^{13}C NMR (125 MHz, MeOD, 298.0 K, δ [ppm]): 23.1, 26.7, 28.8, 40.0, 53.8, 63.0, 65.3, 67.1, 71.0, 105.7, 118.5, 122.1, 124.2, 126.2 (q, J = 269.9 Hz, 1C), 128.1 (q, J = 2.5 Hz, 2C), 128.4, 132.8, 133.9, 134.4 (q, J = 32.3 Hz, 1H), 136.6 (2C), 139.5, 144.9, 146.2, 148.6, 158.9; IR (ATR): 3182, 1620, 1323, 1116, 1066, 897, 863 cm^{-1}; HRMS (API) calcd for [$C_{27}H_{28}F_3N_2O_2^+$] 469.2097, found 401.2090.

Catalyst QNOH-3. Catalyst **QNOH-3**: by following the general procedure, starting from 6′-demethylated quinine (334 mg, 1.08 mmol) and 9-(chloromethyl)anthracene (267 mg, 1.18 mmol) as yellow solid (523 mg, 0.97 mmol, 90%). Mp = 186–190 °C; $[\alpha]_D$ = −89.3° (c = 1.0, MeOH, 23 °C); ^{1}H NMR (500 MHz, MeOD, 298.0 K, δ [ppm]): 1.49–1.65 (m, 2H), 1.93–1.98 (m, 1H), 2.14–2.23 (m, 1H), 2.14–2.23 (m, 1H), 2.31–2.37 (m, 1H), 2.43–2.50 (m, 1H), 2.79–2.88 (m, 1H), 3.22–3.29 (m, 1H), 3.80–3.87 (m, 1H), 4.40–4.47 (m, 1H), 4.64–4.72 (m, 1H), 5.03 (dd, J_{AC} = 10.5 Hz, J_{AB} = 1.2 Hz, 1H), 5.08 (dd, J_{BC} = 17.2 Hz, J_{AB} = 1.2 Hz, 1H), 5.75 (ddd, J_{BC} = 17.2 Hz, J_{AC} = 10.5 Hz, J_{CX} = 7.1 Hz, 1H), 5.92 (d, J = 14.0 Hz, 1H), 6.49 (d, J = 14.0 Hz, 1H), 6.95 (s, 1H), 7.49 (dd, J = 2.2 Hz, J = 9.2 Hz, 1H), 7.63–7.68 (m, 2H), 6.78 (d, J = 2.2 Hz, 1H), 7.79–7.85 (m, 2H), 7.98 (d, J = 4.5 Hz, 1H), 8.05 (d, J = 9.1 Hz, 1H), 8.24 (d, J = 8.4 Hz, 2H), 8.62 (d, J = 9.1 Hz, 1H), 8.78–8.83 (m, 2H), 8.56 (s, 1H); ^{13}C NMR (125 MHz, MeOD, 298.0 K, δ [ppm]): 23.6, 27.1, 28.2, 40.6, 54.3, 57.8, 64.4, 67.9, 70.9, 106.0, 118.5, 120.0, 122.3, 124.3, 125.9, 126.4, 127.4, 127.5, 128.5, 130.1, 130.2, 132.0, 132.0, 132.8, 133.9, 133.9, 134.6, 135.5, 135.6, 139.6, 144.9, 146.4, 148.6, 159.0; IR (ATR): 3077, 2362, 1619, 1464, 1224, 858, 738 cm^{-1}; HRMS (API) calcd for [$C_{34}H_{33}N_2O_2^+$] 501.2537, found 501.2528.

Catalyst QDOH-1. Catalyst **QDOH-1**: by following the general procedure, starting from 6′-demethylated quinidine (100 mg, 0.32 mmol) and benzyl bromide (40 μL, 57, 5 mg, 0.34 mmol). Beige solid (108 mg, 0.22 mmol, 70%). Mp > 200 °C; $[\alpha]_D$ = +169.2° (c = 0.5, MeOH, 15 °C); ^{1}H NMR (300 MHz, CD_3OD, 298.0 K, δ [ppm]): 1.13–1.17 (m, 1H), 1.88–1.96 (m, 3H), 2.45–2.67 (m, 2H), 3.04–3.16 (m, 1H), 3.58–3.67 (m, 1H), 3.88–4.04 (m, 2H), 4.66 (bs, 1H), 5.24–5.30 (m, 2H), 6.00–6.14 (m, 1H), 6.46 (bs, 2H), 7.40 (d, J = 7.5 Hz, 1H), 7.59–7.99 (m, 9H), 8.72 (d, J = 5.0 Hz, 1H). ^{13}C NMR (60 MHz, CD_3OD, 298.0 K, δ [ppm]): 20.7; 23.3; 27.1; 37.5; 54.3; 56.8; 63.4; 65.4; 67.6; 103.7; 116.6; 119.7; 122.0; 126.1; 127.2; 129.1 (2C); 130.4 (2C); 133.5 (2C); 136.3; 142.5; 146.3; 156.6.

Catalyst QDOH-2. Catalyst **QDOH-2**: spectra and analytical data as reported.[13a]

Catalyst QDOH-3. Catalyst **QDOH-3**: by following the general procedure, starting from 6′-demethylated quinidine (93 mg, 0.3 mmol) and 1-(chloromethyl)benzotriazole (54 mg, 0.32 mmol). Beige solid (75 mg, 63%) mp > 200 °C; $[\alpha]_D$ = +213.9° (c = 0.5, MeOH, 15 °C); ^{1}H NMR (300 MHz, $CDCl_3$, 298.0 K, δ [ppm]): 0.86–1.00 (m, 1H), 1.60–1.98 (m, 3H), 2.09–2.39 (m, 2H), 2.59–2.86 (m, 1H), 3.12–3.49 (m, 1H), 4.06–4.46 (m, 2H), 4.59–4.79 (m, 1H), 5.06–5.30 (m, 2H), 5.74–5.93 (m, 1H), 6.43 (bs, 2H), 6.81 (d, J = 9.2 Hz, 1H), 7.13–7.25 (m, 3H), 7.31–7.45 (m, 1H), 7.46–7.74 (m, 4H), 7.91 (s, 1H), 8.48 (d, J = 8.5 Hz, 1H), 8.64 (d, J = 4.5 Hz, 1H). ^{13}C NMR (75 MHz, $CDCl_3$, 298.0 K, δ [ppm]): 21.2; 23.6; 26.6; 37.8; 54.1; 57.0; 65.8; 66.6; 67.7; 103.2; 110.6; 118.6; 119.2; 119.8; 121.2; 124.3; 125.0; 129.8; 131.2; 133.7; 134.5; 140.7; 142.5; 144.7; 146.6; 156.1.

General procedure for the synthesis of isoindolinones 3 under phase transfer catalyzed conditions

In a round-bottom flask, amine **2** (0.11 eq., 0.11 mmol) was added at room temperature to a stirred solution of 2-formylbenzonitrile **1** (0.10 mmol), K_2CO_3 (1 eq., 0.1 mmol) and phase transfer catalyst **QNOH-1** (8% mol) in CH_2Cl_2 (1.8 mL). The mixture was stirred until starting material disappeared (8–18 h), then the solvent was removed under reduced pressure and the residue purified by flash chromatography on silica gel with hexane–ethyl acetate 1 : 1 mixtures.

3-(Benzylamino)isoindolin-1-one (3aa). $[\alpha]_D$ = −63.7° (e.r. = 99 : 1, c = 0.5, $CHCl_3$, 22 °C). Spectra and analytical data as reported.[7] HPLC: Chiral pack AD column, hexane–^{i}PrOH 8 : 2, 0.6 mL min^{-1}, λ = 254 nm (t_{minor} = 12.5 min, t_{major} = 15.7 min).

3-((4-Chlorobenzyl)amino)isoindolin-1-one (3ab). $[\alpha]_D$ = −55.2° (e.r. = 95 : 5, c = 0.5, $CHCl_3$, 17 °C). Spectra and analytical data as reported.[7] HPLC: Chiralpack AD column, hexane–^{i}PrOH 8 : 2, 0.6 mL min^{-1}, λ = 254 nm (t_{minor} = 15.5 min, t_{major} = 16.6 min).

3-((2-Methoxybenzyl)amino)isoindolin-1-one (3ac). White amorphous solid; ^{1}H NMR (250 MHz, $CDCl_3$): 7.81 (1H, d, J = 7.5 Hz); 7.59–7.46 (3H, m); 7.28–7.25 (2H, m); 6.97–6.87 (2H, m); 6.36 (1H, s); 5.47 (1H, s); 4.02 (1H, d, J = 12.5 Hz); 3.84 (3H, s); 3.72 (1H, d, J = 12.5 Hz); 1.76 (1H, bs). ^{13}C NMR (60 MHz, $CDCl_3$): 169.8; 157.5; 145.7; 132.1; 132.0; 129.7; 129.1; 128.9; 128.0; 123.8; 123.3; 120.9; 110.5; 70.7; 55.3.3; 43.3. MS (ESI): m/z = 291 (M + Na$^+$). Anal. calcd for $C_{16}H_{16}N_2O_2$: C, 71.62; H, 6.01; N, 10.44; O, 11.93. Found: C, 71.65; H, 6.03; N, 10.41. HPLC: Chiralpack AD column, hexane–^{i}PrOH 8 : 2, 0.6 mL min^{-1}, λ = 254 nm (t_{minor} = 13.0 min, t_{major} = 15.7 min).

3-(Propylamino)isoindolin-1-one (3ad). White amorphous solid; ^{1}H NMR (250 MHz, $CDCl_3$): 7.81 (1H, d, J = 5.0 Hz); 7.59–7.50 (3H, m); 6.92 (1H, bs); 5.49 (1H, bd); 2.67–2.60 (1H, m); 2.60–2.49 (1H, m); 1.69 (1H, bs) 1.53–1.45 (2H, m), 0.91 (3H, t, J = 7.5 Hz). ^{13}C NMR (60 MHz, $CDCl_3$): 170.1; 145.6; 132.2; 132.0; 129.1; 123.6; 123.4; 70.5; 46.3; 23.6; 11.6. MS (ESI): m/z = 191 (M + H$^+$). Anal. calcd for $C_{11}H_{14}N_2O$: C, 69.45; H, 7.42; N, 14.73; O, 8.41. Found: C, 69.48; H, 7.44; N, 14.70. HPLC: Chiralpack AD column, hexane–^{i}PrOH 8 : 2, 0.6 mL min^{-1}, λ = 254 nm (t_{minor} = 9.0 min, t_{major} = 11.3 min).

3-(Benzylamino)-6-bromoisoindolin-1-one (3ba). $[\alpha]_D$ = −31.5° (e.r. = 98 : 2, c = 0.4, $CHCl_3$, 19 °C). Spectra and analytical data as reported.[7] HPLC: Chiralpack AD column, hexane–^{i}PrOH 8 : 2, 0.6 mL min^{-1}, λ = 254 nm (t_{minor} = 13.0 min, t_{major} = 15.7 min).

6-Bromo-3-((4-chlorobenzyl)amino)isoindolin-1-one (3bb). $[\alpha]_D$ = −64.4° (e.r. = 93 : 7, c = 0.8, $CHCl_3$, 19 °C). Pale yellow amorphous solid; ^{1}H NMR (300 MHz, $CDCl_3$): 7.94 (1H, s); 7.72–7.68 (1H, m); 7.52–7.46 (2H, m); 7.28–7.26 (3H, m); 5.49 (1H, s); 4.03 (1H, bs); 3.85 (1H, d, J = 13.3 Hz); 3.71 (1H, d, J = 13.3 Hz); 2.28 (1H, bs). ^{13}C NMR (75 MHz, $CDCl_3$): 143.9; 137.7; 135.3; 134.1; 133.1; 129.4; 128.7; 126.7; 125.4; 123.5; 69.8; 47.8. MS

(ESI): $m/z = 273$ ($M + H^+$). Anal. calcd for $C_{15}H_{13}ClN_2O$: C, 66.06; H, 4.80; Cl, 13.00; N, 10.27; O, 5.87. HPLC: Chiralpack AD column, hexane–^{i}PrOH 8 : 2, 0.6 mL min^{-1}, $\lambda = 254$ nm ($t_{major} = 18.3$ min, $t_{minor} = 23.4$ min).

6-Bromo-3-((2-methoxybenzyl)amino)isoindolin-1-one (3bc). White amorphous solid; ^{1}H NMR (250 MHz, $CDCl_3$): 7.92 (1H, s); 7.70–7.66 (1H, m); 7.46–7.43 (1H, m); 7.28–7.23 (2H, m); 6.98–6.87 (2H, m); 6.39 (1H, bs); 5.42 (1H, s); 4.01 (1H, d, $J = 12.5$ Hz); 3.83 (3H, s); 3.70 (1H, d, $J = 12.5$ Hz); 1.70 (1H, bs). ^{13}C NMR (75 MHz, $CDCl_3$): 168.2; 157.4; 144.3; 135.1; 134.0; 129.7; 129.0; 127.8; 126.5; 125.5; 123.2; 120.9; 110.6; 70.5; 55.3; 45.2. MS (ESI): $m/z = 385$ ($M + K^+$). Anal. calcd for $C_{16}H_{15}BrN_2O_2$: C, 55.35; H, 4.35; Br, 23.01; N, 8.07; O, 9.22. Found: C, 55.38; H, 4.35; Br, 22.09; N, 8.05. HPLC: Chiralpack AD column, hexane–^{i}PrOH 8 : 2, 0.6 mL min^{-1}, $\lambda = 254$ nm ($t_{minor} = 12.7$ min, $t_{major} = 17.0$ min).

3-(Benzylamino)-6-methoxyisoindolin-1-one (3ca). White amorphous solid; ^{1}H NMR (400 MHz, $CDCl_3$): 7.50 (1H, d, $J = 8$ Hz); 7.34–7.14 (6H, m); 7.12 (1H, d, $J = 4.0$ Hz); 6.52 (1H, s); 5.49 (1H, s); 3.89 (1H, d, $J = 12$ Hz); 3.87 (3H, s); 3.75 (1H, d, $J = 12$ Hz); 1.61 (1H, bs). ^{13}C NMR (100 MHz, $CDCl_3$): 170.1; 160.9; 139.6; 137.5; 133.5; 128.6 (2C); 128.1 (2C); 127.4; 124.6; 120.3; 106.3; 69.9; 55.7; 48.7. MS (ESI): $m/z = 307$ ($M + K^+$). Anal. calcd for $C_{16}H_{16}N_2O_2$: C, 71.62; H, 6.01; N, 10.44; O, 11.93. Found: C, 71.64; H, 6.04; N, 10.42; HPLC: Chiralpack AD column, hexane–^{i}PrOH 8 : 2, 0.6 mL min^{-1}, $\lambda = 254$ nm ($t_{minor} = 14.4$ min, $t_{major} = 19.7$ min).

3-(Benzylamino)-6-fluoroisoindolin-1-one (3da). White amorphous solid; ^{1}H NMR (300 MHz, $CDCl_3$): 7.59 (1H, dd, $J_{AC} = 9.0$ Hz, $J_{AB} = 3.0$ Hz); 7.49–7.47 (1H, m); 7.35–7.25 (6H, m); 6.90 (1H, s); 5.50 (1H, s); 3.90 (1H, d, $J = 12$ Hz); 3.75 (1H, d, $J = 12$ Hz); 1.96 (1H, bs). ^{13}C NMR (75 MHz, $CDCl_3$): 168.8; 163.5 (1C, d, $J'_{FC} = 246$ Hz); 140.7; 139.3; 134.1 (1C, d, $J'''_{FC} = 9$ Hz); 128.7 (2C); 128.1 (2C); 127.5; 125.4 (1C, d, $J'''_{FC} = 8$ Hz); 119.7 (1C, d, $J''_{FC} = 23$ Hz); 110.3 (1C, d, $J''_{FC} = 23$ Hz); 69.8; 48.8. MS (ESI): $m/z = 257$ ($M + H^+$). Anal. calcd for $C_{15}H_{13}FN_2O$: C, 70.30; H, 5.11; F, 7.41; N, 10.93; O, 6.24. Found: C, 70.32; H, 5.10; F, 7.39; N, 10.91. HPLC: Chiralpack AD column, hexane–^{i}PrOH 8 : 2, 0.6 mL min^{-1}, $\lambda = 254$ nm ($t_{minor} = 11.0$ min, $t_{major} = 12.7$ min).

3-(Benzylamino)-6-chloroisoindolin-1-one (3ea). $[\alpha]_D = -103.9°$ (e.r. = 90 : 10, $c = 0.5$, $CHCl_3$, 17 °C). White amorphous solid; ^{1}H NMR (400 MHz, $CDCl_3$): 7.79 (1H, s); 7.56 (2H, bs); 7.34–7.28 (5H, m); 5.53 (1H, s); 3.90 (1H, d, $J = 13.0$ Hz); 3.75 (1H, d, $J = 13.0$ Hz); 1.98 (1H, bs). ^{13}C NMR (100 MHz, $CDCl_3$): 168.9; 143.6; 139.3; 135.6; 133.9; 132.5; 128.6 (2C); 128.1 (2C); 127.5; 125.1; 123.7; 69.8; 48.8 MS (ESI): $m/z = 295$ ($M + Na^+$). Anal. calcd for $C_{15}H_{13}ClN_2O$: C, 66.06; H, 4.80; Cl, 13.00; N, 10.27; O, 5.87. Found: C, 66.09; H, 4.82; Cl, 12.96; N, 10.25. HPLC: Chiralpack AD column, hexane–^{i}PrOH 8 : 2, 0.6 mL min^{-1}, $\lambda = 254$ nm ($t_{minor} = 13.9$ min, $t_{major} = 16.4$ min).

(*R*)-3-(((*S*)-1-Phenylethyl)amino)isoindolin-1-one (3af). $[\alpha]_D = -137.0°$ ($c = 0.5$, $CHCl_3$, 17 °C). Spectra and analytical data as reported.[7]

(*R*)-3-(((*R*)-1-Phenylethyl)amino)isoindolin-1-one (3af). $[\alpha]_D = -57.1°$ ($c = 0.5$, $CHCl_3$, 17 °C). Spectra and analytical data as reported.[7]

Computational procedure

Conformer search for the **QNOH-1** ammonium cation, intermediate **A** and **3af** (*RR* and *RS* diastereoisomers) was carried out by using the MMFF94 force field as implemented in Spartan.[22] Different starting structures were considered for each system and both the systematic and the Montecarlo based algorithms were employed. All the conformers up to 10 kcal mol^{-1} with respect to minimum energy structures were then optimized by quantum chemical computations using density functional theory (DFT). Guess structures of the ion pair consisting of catalyst **QNOH-1** and intermediate **A** were obtained by docking simulations employing a homemade program; the starting geometries of the catalyst and the ligand were initially optimized at the MMFF94 level. Geometry optimizations and Hessian computations needed to ascertain the nature of the stationary points were carried out by using the M06-2X functional which is known to provide reliable geometries and barrier heights especially for large systems.[23] The 6-31G(d) basis set was used in optimizations; single point computations with the 6-311+G(d,p) basis set were carried out to obtain accurate energies. Intrinsic reaction coordinate (IRC) calculations were performed to check the connectivity of all the TS with their corresponding minima. All the TS's exhibit only one large imaginary frequency corresponding to the stretching coordinate of the forming bond, while the minimum energy structures have only positive eigenvalues of the Hessian matrix. Solvent effects were taken into account by means of the polarizable continuum model (PCM) which was included in all computations.[24] All the quoted energies refer to 6-311+G(d,p) basis set; they include zero point vibrational corrections (computed at the 6-31G(d) level) and the solvent polarization contribution. Atomic charges were estimated by the atomic polar tensor approach (APT).[25] DFT computations were carried out by using the Gaussian program.[26]

Although entropic contributions are expected to be significant for association processes, their effects should elide in differences, the quantities that really matter. Therefore our discussion has been based on internal energies, following the same arguments given in ref. 27.

NMR computations for the *RS*/*RR* diastereomers of **3af** were carried out by following the procedure of ref. 28: the minimum energy configurations and the energetics needed for the Boltzmann weighting of the shielding tensors were taken from PCM($CHCl_3$)/M06-2X/6-31+G(d,p) calculations, while shielding tensors were calculated at the PCM($CHCl_3$)/B3LYP/6-311+G(2d,p) level.

Conclusions

The first asymmetric route to chiral N-Mannich bases of 1-isoindolinones has been successfully opened by using a readily available bifunctional cinchona-derivative ammonium salt as phase transfer catalyst in the presence of K_2CO_3 as base. The goal was achieved thanks to an efficient cascade reaction of 2-formylbenzonitriles and primary amines involving an uncommon enantioselective aza-Mannich rearrangement step.

Theoretical computations show that **QNOH-1** acts as bifunctional catalyst determining the enantio-sense of the aza-Mannich step through the establishment of an effective network of hydrogen bonds.

Acknowledgements

This research was funded by Region Campania under POR Campania FESR 2007–2013 – O.O. 2.1 (FarmaBioNet). The financial support of the University of Salerno is gratefully acknowledged.

Notes and references

1 (*a*) H. Kawagishi, M. Ando and T. Mizuno, *Tetrahedron Lett.*, 1990, **31**, 373; (*b*) S. F. Hinkley, J. C. Fettinger, K. Dudley and B. B. Jarvis, *J. Antibiot.*, 1999, **52**, 988; (*c*) M. Jacolot, M. Jean, N. Tumma, A. Bondon, S. Chandrasekhar and P. Van de Weghe, *J. Org. Chem.*, 2013, **78**, 7169; (*d*) E. Li, L. Jiang, L. Guo, H. Zhang and Y. Che, *Bioorg. Med. Chem.*, 2008, **16**, 7894; (*e*) N. Slavov, J. Cvengroš, J. M. Neudörfl and H.-G. Schmalz, *Angew. Chem., Int. Ed.*, 2010, **49**, 7588.

2 (*a*) I. Takahashi, T. Kawakami, E. Hirano, H. Yokota and H. Kitajima, *Synlett*, 1996, 353; (*b*) t. L. Stuk, B. K. Assink, R. C. Bates Jr, T. R. Erdman, V. Fedij, S. M. Jennings, J. L. Lassig, R. J. Smith and L. T. Smith, *Org. Process Res. Dev.*, 2003, **7**, 851; (*c*) E. Van der Kleijn, *Eur. J. Clin. Pharmacol.*, 1989, **36**, 247.

3 (*a*) H. A. Priestap, *Phytochemistry*, 1985, **24**, 848; (*b*) A. Couture, E. Deniau, P. Grandclaudon and C. Hoarau, *J. Org. Chem.*, 1998, **63**, 3128; (*c*) A. Mertens, J. H. Zilch, B. Konig, W. Schafer, T. Poll, W. Kampe, H. Seidel, U. Leser and H. Leinert, *J. Med. Chem.*, 1993, **36**, 2526; (*d*) A. Bjoere, *et al*. WO2008008022, 2008.

4 For recent reviews on the synthesis of isoindolinones, see: (*a*) A. Di Mola, L. Palombi and A. Massa, *Targets Heterocycl. Syst.*, 2014, **18**, 113; (*b*) K. Speck and T. Magauer, *Beilstein J. Org. Chem.*, 2013, **9**, 2048.

5 (*a*) A. Di Mola, M. Tiffner, F. Scorzelli, L. Palombi, R. Filosa, P. De Caprariis, M. Waser and A. Massa, *Beilstein J. Org. Chem.*, 2015, **11**, 2591; (*b*) M. Perillo, A. Di Mola, R. Filosa, L. Palombi and A. Massa, *RSC Adv.*, 2014, **4**, 4239; (*c*) C. Petronzi, S. Collarile, G. Croce, R. Filosa, P. De Caprariis, A. Peduto, L. Palombi, V. Intintoli, A. Di Mola and A. Massa, *Eur. J. Org. Chem.*, 2012, 5357; (*d*) V. More, R. Rohlmann, O. G. Mancheno, C. Petronzi, L. Palombi, A. De Rosa, A. Di Mola and A. Massa, *RSC Adv.*, 2012, **2**, 3592.

6 (*a*) L. Palombi, A. Di Mola, C. Vignes and A. Massa, *Mol. Diversity*, 2014, **18**, 323; (*b*) P. Antico, V. Capaccio, A. Di Mola, A. Massa and L. Palombi, *Adv. Synth. Catal.*, 2012, **354**, 1717.

7 L. Palombi, A. Di Mola and A. Massa, *New J. Chem.*, 2015, **39**, 81.

8 (*a*) M. J. O'Donnell, W. D. Bennett and S. Wu, *J. Am. Chem. Soc.*, 1989, **111**, 2353; (*b*) E. J. Corey, F. Xu and M. C. Noe, *J. Am. Chem. Soc.*, 1997, **119**, 12414; (*c*) R. Helder, J. C. Hummelen, R. W. P. M. Laane, J. S. Wiering and H. Wynberg, *Tetrahedron Lett.*, 1976, **17**, 1831–1834; (*d*) U. H. Dolling, P. Davis and E. J. J. Grabowski, *J. Am. Chem. Soc.*, 1984, **106**, 446–447.

9 For recent reviews on chiral phase transfer catalysts see: (*a*) S. Kaneko, Y. Kumatabara and S. Shirakawa, *Org. Biomol. Chem.*, 2016, DOI: 10.1039/c5ob02446c; (*b*) S. Shirakawa and K. Maruoka, *Angew. Chem., Int. Ed.*, 2013, **52**, 4312; (*c*) S.-s. Jew and H.-g. Park, *Chem. Commun.*, 2009, 7090; (*d*) *Asymmetric Phase Transfer Catalysis*, K. Maruoka, ed. Wiley-VCH, Weinheim, 2008; (*e*) K. Maruoka, *Chem. Rec.*, 2010, **10**, 254.

10 For selected recent examples, see: (*a*) R. Herchl and M. Waser, *Tetrahedron*, 2014, **70**, 1935–1960; (*b*) J. Novacek and M. Waser, *Eur. J. Org. Chem.*, 2013, 637–648; (*c*) R. Herchl and M. Waser, *Tetrahedron Lett.*, 2013, **54**, 2472; (*d*) K. M. Johnson, M. S. Rattley, F. Sladojevich, D. M. Barber, M. G. Nuñez, A. M. Goldys and D. J. Dixon, *Org. Lett.*, 2012, **14**, 2492; (*e*) C. D. Fiandra, L. Piras, F. Fini, P. Disetti, M. Moccia and M. F. A. Adamo, *Chem. Commun.*, 2012, **48**, 3863; (*f*) P. Elsner, L. Bernardi, G. Dela Salla, J. Overgaard and K. A. Jørgensen, *J. Am. Chem. Soc.*, 2008, **130**, 4897.

11 (*a*) S. E. Denmark, N. D. Gould and L. M. Wolf, *J. Org. Chem.*, 2011, **76**, 4260; (*b*) S. E. Denmark, N. D. Gould and L. M. Wolf, *J. Org. Chem.*, 2011, **76**, 4337; (*c*) L. Wang, S. Shirakawa and K. Maruoka, *Angew. Chem., Int. Ed.*, 2011, **50**, 5327; (*d*) S. Shirakawa and K. Maruoka, *Tetrahedron Lett.*, 2014, **55**, 3833; (*e*) G. P. Petrova, H.-B. Li, K. Maruoka and K. Morokuma, *J. Phys. Chem. B*, 2014, **118**, 5154.

12 This screening should not be considered exhaustive, since, for brevity, we reported only the most significant experiments.

13 (*a*) A. Berkessel, M. Guixà, F. Schmidt, J. M. Neudörfl and J. Lex, *Chem.–Eur. J.*, 2007, **13**, 4483; (*b*) H.-J. Lee and C.-W. Cho, *J. Org. Chem.*, 2015, **80**, 11435.

14 For a review on bifunctional chiral ammonium salts and leading references see: J. Novacek and M. Waser, *Eur. J. Org. Chem.*, 2014, 802–809.

15 For a book and selected examples see: (*a*) *Enantiomer Separation: Fundamentals and Practical Methods*, ed. Fumio Toda, Kluwer Academic Publishers, Â Dordrecht, Boston, London, 2004; (*b*) W.-W. Chen, M.-H. Xu and G.-Q. Lin, *Tetrahedron Lett.*, 2007, **48**, 7508; (*c*) A. Ishii, M. Kanai, K. Higashiyama and k. Mikami, *Chirality*, 2002, **14**, 709.

16 (*a*) G. K. Surya Prakash, F. Wang, C. Ni, J. Shen, R. Haiges, A. K. Yudin, T. Mathew and G. A. Olah, *J. Am. Chem. Soc.*, 2011, **133**, 9992; (*b*) G. K. Surya Prakash, F. Wang, M. Rahm, Z. Zhang, C. Ni, J. Shen and G. A. Olah, *J. Am. Chem. Soc.*, 2014, **136**, 10418.

17 G. P. Petrova, H.-B. Li, K. Maruoka and K. Morokuma, *J. Phys. Chem. B*, 2014, **118**, 5154.

18 (*a*) D. Uraguchi, K. Koshimoto and T. Ooi, *J. Am. Chem. Soc.*, 2008, **130**, 10878; (*b*) D. Uraguchi, K. Oyaizu and T. Ooi, *Chem.–Eur. J.*, 2012, **18**, 8306.

19 Q. Wang, Q. Wang, B. Zhang, X. Sun and S. Zhang, *Synlett*, 2009, 1311.

20 B. A. Provencher, K. J. Bartelson, Y. Liu, B. M. Foxman and L. Deng, *Angew. Chem., Int. Ed.*, 2011, **50**, 10565.
21 H. Li, Y. Wang, L. Tang and L. Deng, *J. Am. Chem. Soc.*, 2004, **126**, 9906.
22 *Spartan'04*, Wavefunction, Inc., Irvine, CA.
23 S. Schenker, C. Schneider, S. B. Tsogoeva and T. Clark, *J. Chem. Theory Comput.*, 2011, **7**, 3586.
24 S. Miertuš, E. Scrocco and J. Tomasi, *Chem. Phys.*, 1981, **55**, 117.
25 J. Cioslowski, *J. Am. Chem. Soc.*, 1989, **111**, 8333.
26 M. J. Frisch, *et al*. *Gaussian 09 Revision D.01*, Gaussian Inc., Wallingford CT, 2009.
27 (*a*) A. Russo, A. Capobianco, A. Perfetto, A. Lattanzi and A. Peluso, *Eur. J. Org. Chem.*, 2011, 1922; (*b*) A. Capobianco, A. Russo, A. Lattanzi and A. Peluso, *Adv. Synth. Catal.*, 2012, **354**, 2789; (*c*) T. Caruso, A. Capobianco and A. Peluso, *J. Am. Chem. Soc.*, 2007, **129**, 15347.
28 S. Meninno, A. Capobianco, A. Peluso and A. Lattanzi, *Green Chem.*, 2015, **17**, 2317.